

Optimal waveguide dimensions for nonlinear interactions

M. A. Foster, K. D. Moll, and Alexander L. Gaeta

School of Applied and Engineering Physics, Cornell University, Ithaca, NY 14853
maf42@cornell.edu, kdm14@cornell.edu, alg3@cornell.edu

Abstract: We investigate strong light confinement in high core-cladding index contrast waveguides with dimensions comparable to and smaller than the wavelength of incident light. We consider oval and rectangular cross sections and demonstrate that an optimal core size exists that maximizes the effective nonlinearity. We also determine that waveguides with asymmetrical cross sections provide the maximum possible nonlinearity, although only a small improvement over the symmetric case. Furthermore, we find that for a specified waveguide shape the largest nonlinearity occurs for nearly the same core area in all cases. Calculations of the dispersion for the optimal-size waveguide at a particular wavelength indicate that the group-velocity dispersion is normal. Ultimately, such designs could be used to develop low-power all-optical devices and to produce waveguides for ultra-low threshold nonlinear frequency generation such as supercontinuum generation.

© 2004 Optical Society of America

OCIS codes: (190.4370) Nonlinear optics, fibers; (190.4360) Nonlinear optics, devices; (060.2270) Fiber characterization; (250.5300) Photonic integrated circuits

References and links

1. T. A. Birks and Y. W. Li, "The shape of fiber tapers," *J. Lightwave Technol.* **10**, 432–438 (1992).
2. J. K. Ranka, R. S. Windeler, and A. J. Stentz, "Visible continuum generation in air-silica microstructure optical fibers with anomalous dispersion at 800 nm," *Opt. Lett.* **25**, 25–27 (2000).
3. W. J. Wadsworth, A. Ortigosa-Blanch, J. C. Knight, T. A. Birks, T. P. M. Man, and P. St.J. Russell, "Supercontinuum generation in photonic crystal fibers and optical fiber tapers: a novel light source," *J. Opt. Soc. Am. B* **19**, 2148–2155 (2002).
4. J. C. Knight, "Photonic crystal fibres," *Nature* **424**, 847–851 (2003).
5. P. St.J. Russell, "Photonic crystal fibers," *Science* **299**, 358–362 (2003).
6. L. M. Tong, R. R. Gattass, J. B. Ashcom, S. L. He, J. Y. Lou, M. Y. Shen, I. Maxwell, and E. Mazur, "Subwavelength-diameter silica wires for low-loss optical wave guiding," *Nature* **426**, 816–819 (2003).
7. V. R. Almeida, R. R. Panepucci, and M. Lipson, "Nanotaper for compact mode conversion," *Opt. Lett.* **28**, 1302–1304 (2003).
8. A. W. Snyder and J. D. Love, *Optical Waveguide Theory* (Kluwer Academic Publishers, 1983).
9. C. R. Pollock and M. Lipson, *Integrated Photonics* (Kluwer Academic Publishers, 2003).
10. J. K. Ranka, R. S. Windeler, and A. J. Stentz, "Optical properties of high-delta air-silica microstructure optical fibers," *Opt. Lett.* **25**, 796–798 (2000).
11. M. Artiglia, G. Coppa, P. Divita, M. Potenza, and A. Sharma, "Mode field diameter measurements in single-mode optical fibers," *J. Lightwave Tech.* **7**, 1139–1152 (1989).
12. G. P. Agrawal, *Nonlinear Fiber Optics* (Academic Press, 1989).
13. D. Akimov, M. Schmitt, R. Maksimenka, K. Dukel'skii, Y. Kondrat'ev, A. Khokhlov, V. Shevandin, W. Kiefer, and A. M. Zheltikov, "Supercontinuum generation in a multiple-submicron-core microstructure fiber: toward limiting waveguide enhancement of nonlinear-optical processes," *Appl. Phys. B* **77**, 299–305 (2003).
14. A. M. Zheltikov, "The physical limit for the waveguide enhancement of nonlinear-optical processes," *Optics and Spectroscopy* **95**, 410–415 (2003).

15. P. Dumais, F. Gonthier, S. Lacroix, A. Villeneuve, P. G. J. Wigley, and G. I. Stegeman, "Enhanced self-phase modulation in tapered fibers," *Opt. Lett.* **18**, 1996–1998 (1993).
 16. V. Finazzi, T. M. Monro, and D. J. Richardson, "The role of confinement loss in highly nonlinear silica holey fibers," *IEEE Photon. Technol. Lett.* **15**, 1246–1248 (2003).
 17. S. Johnson and J. D. Joannopoulos, "Block-iterative frequency-domain methods for Maxwell's equations in a planewave basis," *Opt. Express* **8**, 173–190 (2001), <http://www.opticsexpress.org/abstract.cfm?URI=OPEX-8-3-173>.
 18. L. M. Tong, J. Y. Lou, and E. Mazur, "Single-mode properties of sub-wavelength-diameter silica and silicon wire waveguides," *Opt. Express* **12**, 1025–1035 (2004), <http://www.opticsexpress.org/abstract.cfm?URI=OPEX-12-6-1025>.
 19. J. C. Knight, J. Arriaga, T. A. Birks, A. Ortigosa-Blanch, W. J. Wadsworth, and P. St.J. Russell, "Anomalous dispersion in photonic crystal fiber," *IEEE Photon. Technol. Lett.* **12**, 807–809 (2000).
 20. D. Ouzounov, D. Homoelle, W. Zipfel, W. W. Webb, A. L. Gaeta, J. A. West, J. C. Fajardo, and K. W. Koch, "Dispersion measurements of microstructured fibers using femtosecond laser pulses," *Opt. Commun.* **192**, 219–223 (2001).
 21. W. H. Reeves, J. C. Knight, P. St.J. Russell, and P. J. Roberts, "Demonstration of ultra-flattened dispersion in photonic crystal fibers," *Opt. Express* **10**, 609–613 (2002), <http://www.opticsexpress.org/abstract.cfm?URI=OPEX-10-14-6095>.
 22. W. H. Reeves, D. V. Skryabin, F. Biancalana, J. C. Knight, P. St.J. Russell, F. G. Omenetto, A. Efimov, and A. J. Taylor, "Transformation and control of ultra-short pulses in dispersion-engineered photonic crystal fibres," *Nature* **424**, 511–515 (2003).
-

1. Introduction

For many nonlinear optical processes it is desirable to maximize the product of the intensity and the interaction length. Although focusing the field in a bulk medium increases the field intensity, the interaction length, as defined by the confocal parameter, decreases proportionally. To truly take advantage of small modal areas at a fixed power, guiding structures are necessary to counteract the diffraction inherent to free-space propagation. By decreasing the size of the guiding core and increasing the core-cladding index difference, the mode of an optical waveguide becomes tightly confined, yielding a corresponding increase in the peak intensity. Waveguide devices for supercontinuum generation such as tapered and microstructured fibers take advantage of this effect [1, 2, 3, 4, 5]. These waveguides have large core-cladding index contrast, and most experiments have been performed with core diameters of $\sim 2 \mu\text{m}$. The efficiency of these devices is further enhanced by the shift of the zero group-velocity dispersion (GVD) point to close to the operating wavelengths of femtosecond sources (e.g., Ti-Sapphire), allowing for extended effective interaction lengths. Recently, fabrication of waveguides with core diameters on the order of hundreds of nanometers was demonstrated, and these waveguides were shown to guide light through very small bend radii with minimal loss [6]. As the core decreases in size, the amount of power in the evanescent field increases and eventually exceeds the power in the core [7]. This change in power localization leads to lower peak intensities in the nonlinear core region despite reduced core sizes.

In this paper, we investigate the balance between core size and power confinement for high core-cladding index contrast waveguides with the aim of maximizing nonlinear interactions in these waveguides. We find that the optimal core size is sub-wavelength and that structures with asymmetric cross-sections maximize the effective nonlinearity. We also determine the total dispersion of a fiber for these maximal conditions and find that the GVD of the mode is always normal. Ultimately the design parameters determined by our results could facilitate the development of low-power nonlinear optical switches and waveguides for ultra-low threshold nonlinear optical processes such as supercontinuum generation.

2. Analytical investigation

In our analytical studies, we consider the fundamental mode of circular and symmetric planar slab dielectric waveguides. Analysis of the waveguides consists of numerically solving the transcendental characteristic equation for the propagation wavevectors [8, 9]. Solving for the first root of these equations yields the parameters for the fundamental mode. Unlike the higher-order modes, the fundamental mode of spatially symmetric waveguides has no cutoff condition, and it is always possible to find at least one root of the characteristic equation.

With knowledge of the propagation parameters, the fundamental mode can be characterized. For the case of high core-cladding index contrast, this mode is robust to the excitation of higher-order modes [10]. For the planar slab waveguide the TE and TM fields are described by cosine functions in the core and an exponential decay in the cladding. Similarly, for the circular waveguide, the electric field of the fundamental HE_{11} mode is described by Bessel functions of the first kind in the core and by Bessel functions of the second kind in the cladding. For this investigation the intensity of light propagating down the waveguide is of interest and is proportional to the longitudinal component of the Poynting vector

$$S_z = (\mathbf{E} \times \mathbf{H}^*)_z. \quad (1)$$

We define the mode field diameter (MFD)[11] as

$$\text{MFD} = 2\sqrt{2} \sqrt{\frac{\int S_z r^2 d^2\mathbf{r}}{\int S_z d^2\mathbf{r}}}, \quad (2)$$

where the integrals are evaluated over the transverse profile. This definition of the MFD gives the $1/e$ point for a gaussian profile and provides a standard method for calculating the beam width for non-gaussian intensity profiles. The effective nonlinearity of a waveguide is defined by the nonlinear parameter γ as [12],

$$\gamma = \frac{2\pi}{\lambda} \frac{\int n_2 S_z^2 d^2\mathbf{r}}{(\int S_z d^2\mathbf{r})^2}, \quad (3)$$

where n_2 is the nonlinear index of refraction, λ is the wavelength of propagating light, and the integrals are evaluated over the transverse profile. In our calculations, we assume that the n_2 of the cladding material (e.g., air) is negligible compared to that of the core so the integral in the numerator is evaluated only over the core region.

We investigated several structures of experimental interest. A circular dielectric waveguide with a core index of refraction $n_{core} = 1.45$ and a cladding index of refraction $n_{clad} = 1$ was used to model a glass fiber in air. This geometry describes microstructured fibers with high air-filling fractions and tapered fibers which are both used for supercontinuum generation. Figure 1(a) shows the power localization as the core diameter or wavelength λ is varied. For $\lambda = 0.8 \mu\text{m}$, a core size of 408 nm yields equal distribution of power between the core and cladding. For smaller core diameters the fraction of power contained in the air cladding greatly exceeds that in the core.

The MFD is plotted in Fig. 1(b) as a function of the core diameter and laser wavelength, and we find the existence of three distinct regimes. For cores larger than the wavelength, the MFD scales linearly with wavelength. As the core size becomes comparable to the wavelength, the MFD approaches a minimum, and further decreases in the core size results in a rapidly increasing MFD. In this latter region, the mode is characterized primarily by an exponentially decaying radial profile. For $\lambda = 0.8 \mu\text{m}$, the minimum MFD is 653 nm for a core diameter of 592 nm. However since the mode does not maintain a consistent shape as the core size changes, the smallest MFD does not necessarily correspond to the optimal nonlinearity.

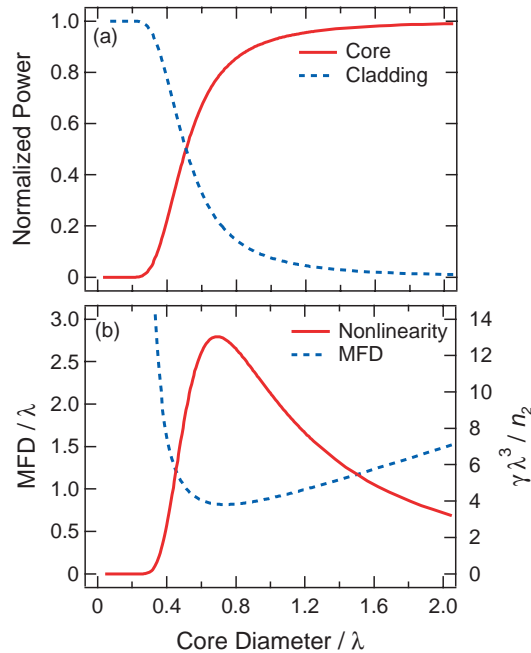


Fig. 1. (a) Power localization and (b) the effective nonlinearity and mode field diameter (MFD) for a circular glass ($n_{core} = 1.45$) waveguide in air ($n_{clad} = 1.0$).

The dependence of the effective nonlinear parameter γ is also shown in Fig. 1(b). The results are qualitatively similar to the previously reported behavior of the average core intensity [13, 14] and effective area [15, 16]. The plot shows a distinct peak corresponding to the optimal core diameter for nonlinear interactions. For $\lambda = 0.8 \mu\text{m}$ and $n_2 = 2.6 \times 10^{-20} \text{ m}^2/\text{W}$, the peak value for the nonlinear parameter of $662 \text{ W}^{-1}/\text{km}$ occurs at a core diameter of 554 nm. Presently, the microstructured fibers used for supercontinuum generation have cores with diameters of $\sim 2 \mu\text{m}$. At $\lambda = 0.8 \mu\text{m}$, the nonlinear coefficient of a 2- μm core fiber is $114 \text{ W}^{-1}/\text{km}$. Therefore, using the optimal core size would yield approximately a $6\times$ larger effective nonlinearity at this wavelength.

We next consider the case of planar slab dielectric waveguides. First, a planar waveguide with $n_{core} = 3.45$ and $n_{clad} = 1.45$ was investigated. This structure corresponds to a Si slab sandwiched by a SiO_2 cladding, which is pertinent to photonic chip applications operating in the infrared. The dependence of γ is shown in Fig. 2. Since the modal extent in the unguided direction is unknown, both this width and the total power must be taken into account to find the actual peak nonlinearity. For $\lambda = 1.55 \mu\text{m}$, the peaks of the TE and TM modes occur at core widths of 209 nm and 318 nm respectively. Also as a comparison to the circular results, a planar waveguide with $n_{core} = 1.45$ and $n_{clad} = 1.0$ was analyzed, and the results are also displayed in Fig. 2. For $\lambda = 0.8 \mu\text{m}$, the peaks of the TE and TM modes occur at core widths of 322 nm and 462 nm respectively.

These results reveal the relationship between polarization and confinement. The peak effective nonlinearities of the TE and TM modes are comparable. However, the optimal waveguide widths for each mode suggest that an asymmetric waveguide cross-section is optimal. For example in photonic-chip applications, the optimal design should be a rectangular waveguide where the larger transverse width is along the direction of polarization. No analytical solution exists for rectangular waveguides due to the coupling between the two transverse dimensions,

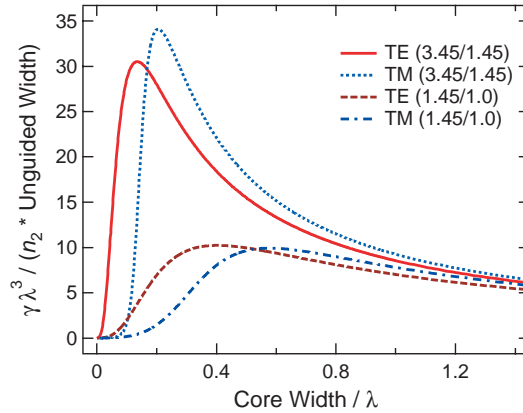


Fig. 2. Effective nonlinearity of the TE and TM modes of a dielectric planar slab waveguide for core/cladding index contrasts of 3.45/1.45 and 1.45/1.0.

that is, the confinement in one dimension influences the confinement in the other dimension so the solution is not separable. Nevertheless, important features can be predicted from our analytic results. As seen in the circular waveguide, a larger optimal size for a two-dimensional guiding structure is to be expected. The added constraining dimension decreases the effective index of the core resulting in a shift to larger optimal core sizes.

Analysis of our results yields the following empirical formulae for the optimal diameter or width scaling for a given operating wavelength and core and cladding indices:

$$\mathcal{D}^{\text{HE}_{11}} = \frac{0.854\lambda}{(n_{\text{core}} + n_{\text{clad}})^{0.6}(n_{\text{core}} - n_{\text{clad}})^{0.4}}, \quad (4)$$

$$\mathcal{W}^{\text{TE}} = \frac{0.422\lambda}{(n_{\text{core}} + n_{\text{clad}})^{0.5}(n_{\text{core}} - n_{\text{clad}})^{0.5}}, \quad (5)$$

$$\mathcal{W}^{\text{TM}} = \frac{0.701\lambda}{(n_{\text{core}} + n_{\text{clad}})^{0.6}(n_{\text{core}} - n_{\text{clad}})^{0.4}}, \quad (6)$$

where $\mathcal{D}^{\text{HE}_{11}}$ is the optimal core diameter for the circular dielectric waveguide, and \mathcal{W}^{TE} and \mathcal{W}^{TM} are the optimal guiding film thicknesses for the TE and TM modes, respectively, of a planar slab waveguide. These approximations accurately predict the optimal core size for most experimentally feasible n_{core} and n_{clad} values to within a few percent.

3. Numerical investigation

For our numerical modeling we use a frequency domain method in a planewave basis similar to that described in Ref. [17]. We first investigate the nonlinear properties of rectangular waveguides with $n_{\text{core}} = 1.45$ and $n_{\text{clad}} = 1.0$ and with $n_{\text{core}} = 3.45$ and $n_{\text{clad}} = 1.45$. Initially, we consider only the mode polarized along the long axis of the rectangular cross-section. The effective nonlinearity as a function of core size and wavelength is shown in Fig. 3 for both of these cases and a range of aspect ratios. The advantage of increasing the core-to-cladding index difference is clearly evident. The waveguide with $n_{\text{core}} = 3.45$ and $n_{\text{clad}} = 1.45$ provides higher mode confinement than that of the waveguide with $n_{\text{core}} = 1.45$ and $n_{\text{clad}} = 1.0$, which yields a $10\times$ larger effective nonlinearity.

Interestingly, the maximum effective nonlinearity for a specific core shape occurs for very nearly the same area in all cases. Therefore, the results of the circular waveguide provide an

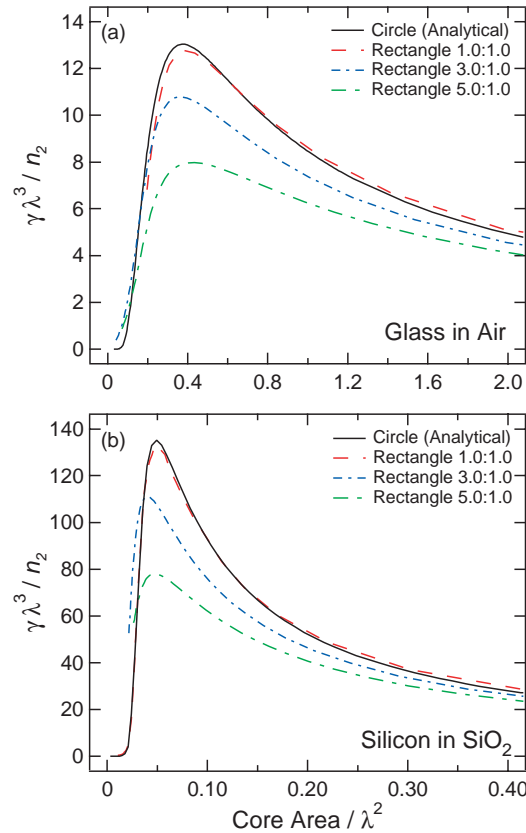


Fig. 3. Effective nonlinearity as a function of core size for the fundamental mode of a circular dielectric waveguide and for rectangular dielectric waveguides with various aspect ratios and core/cladding index contrasts of (a) 1.45/1.0 and (b) 3.45/1.45.

accurate estimate of the core area that produces optimal nonlinearity for any arbitrarily shaped waveguide. Extending the empirical formulae presented previously yields the optimal core area \mathcal{A} for a given operating wavelength and core and cladding indices,

$$\mathcal{A} = \frac{0.573\lambda}{(n_{core} + n_{clad})^{1.2}(n_{core} - n_{clad})^{0.8}}. \quad (7)$$

Although the core area that produces the optimal effective nonlinearity is independent of waveguide shape, the magnitude of the effective nonlinearity at this maximum is highly dependent on shape as shown in Fig. 4. For a given wavelength, the maximum effective nonlinearity occurs at a height-to-width ratio of 1.4 to 1.0 for both sets of refractive indices and the polarization of light along the long axis. This ratio is nearly equal to that predicted by the planar slab investigation. We also consider elliptical core cross-sections, as shown in Fig. 4, and the behavior of an elliptical waveguide is similar to that of a rectangular waveguide with same aspect ratio but displays a slightly larger effective nonlinearity.

While the increase in effective nonlinearity from a slightly asymmetric cross-section is small, this change in shape allows for an inherent nonlinear waveguide birefringence. For a square waveguide, the orthogonally polarized modes are degenerate and yield the same nonlinearity. However for a slightly asymmetric waveguide, the nonlinearity of the mode polarized along the

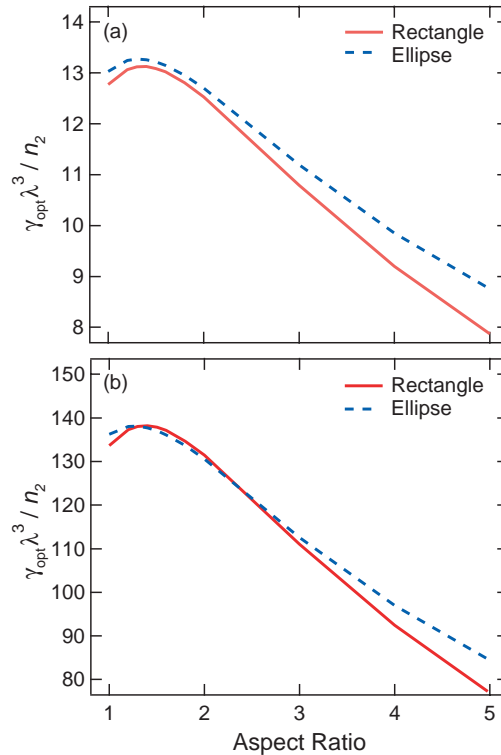


Fig. 4. The optimal effective nonlinearity as a function of core shape for (a) glass ($n_{core} = 1.45$) in air ($n_{clad} = 1.0$) and for (b) Si ($n_{core} = 3.45$) in SiO_2 ($n_{clad} = 1.45$)

long axis of the rectangular cross-section can be 20 percent larger than the short axis polarized mode. This behavior is shown in Fig. 5 for the lowest-order orthogonal modes of a rectangular waveguide.

4. Dispersion

For these highly confining waveguide structures, the waveguide dispersion dominates the inherent dispersion of the material constituents [18, 19, 20, 21, 22]. We investigated the behavior of the GVD for a circular dielectric waveguide with a glass core and an air cladding, and the results are plotted in Fig. 6. For large wavelengths compared to the core diameter, the GVD is nearly zero since the modal power is localized in the air cladding. As shown earlier, the core diameter for optimal nonlinearity of $0.8\text{-}\mu\text{m}$ light is 554 nm . The 600-nm -diameter curve in Fig. 1(a) shows moderate normal dispersion at this wavelength. Interestingly, a peak in the normal GVD occurs at $\lambda = 0.8\text{ }\mu\text{m}$ for a core size of 400 nm , which corresponds to the region where the mode is almost entirely localized in the cladding but still has some measurable power in the core. In contrast, the peak nonlinearity occurs in the region where the mode is mostly confined to the core. Therefore, we find that the peak nonlinearity occurs at larger core sizes than the peak of the normal GVD. Also, for applications where femtosecond pulses are used and operation near the zero-GVD wavelength is desirable, such as supercontinuum generation, it may be preferable to use a fiber structure that is slightly larger than optimal so that the input wavelength is at the zero-GVD point.

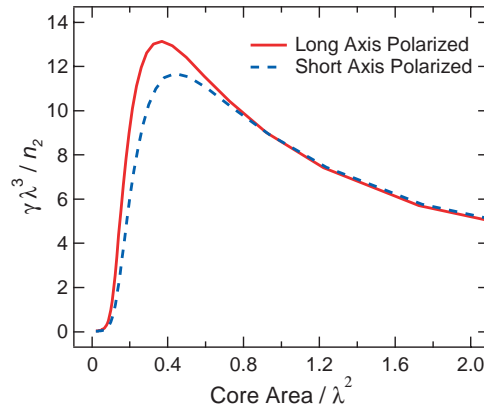


Fig. 5. Effective nonlinearity of the lowest order orthogonally polarized modes of a rectangular waveguide with $n_{core} = 1.45$, $n_{clad} = 1.0$, and an aspect ratio of 1.4 to 1.

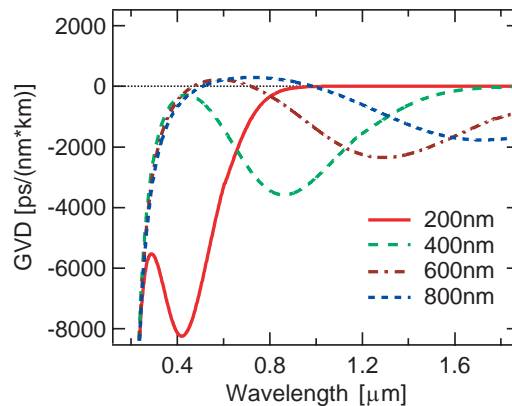


Fig. 6. Group-velocity dispersion of a glass rod in air for core diameters of 200 nm, 400 nm, 600 nm, and 800 nm.

5. Conclusion

We have shown that an optimal waveguide size exists for maximizing the nonlinear coefficient. The optimal size was shown to depend on waveguide geometry and composition. The group velocity dispersion was investigated in the region of optimization showing moderate normal dispersion. Also, a characteristic peak in the GVD was found to occur at smaller core sizes. Minimizing the power needed for nonlinear interactions is of utmost importance for the development of all-optical devices. The designs proposed here provide a basis for producing extremely low-power nonlinear devices. In addition, we expect that such waveguide structures could be utilized to produce supercontinuum generation with significantly lower threshold powers than those associated with currently used microstructured fibers.

This work was supported by the Air Force Office of Scientific Research under contract number F49620-03-1-0223 and by the Center for Nanoscale Systems supported by NSF under award number EEC-0117770.